Applied Water Science (2022) 12: 236
https://doi.org/10.1007/s13201-022-01762-9

ORIGINAL ARTICLE

Characterization of the health and irrigation risks and hydrochemical properties of groundwater: a case study of the Selian coal mine area, Ordos, Inner Mongolia

Yaqiang Li[1] · **Xueliang Zhang**[1]

Received: 3 February 2022 / Accepted: 2 September 2022 / Published online: 17 September 2022

Abstract
Groundwater (GW) is an important source of freshwater in arid and semiarid areas. Some important industrial activities, such as coal mining, also consume GW. There have been few studies evaluating GW quality in the Selian coal mining area of Inner Mongolia. This study aimed to identify the hydrochemical phases and the sources of main ions in the GW of the Selian coal mining area. Water quality analysis was performed on 20 shallow GW samples collected from the study area. Statistical correlation analysis was performed on these water quality data. The quality of irrigation water was evaluated based on water quality indices such as the sodium absorption rate and sodium percentage. The risk of nitrate pollution in the study area to human health was evaluated by GW nitrate content. The results show that the dominant GW chemistry types in the study area are the mixed and Ca–HCO_3 types. Correlation analysis indicates that rock weathering and leaching are the main natural drivers of GW hydrochemistry in this area. The irrigation risk analysis shows that GW in this area can be used for irrigation, although some caution is needed. The human health risk assessment shows that GW nitrate pollution poses more risk to children than to adults by a factor of 1.168. It is recommended that centralized treatment of drinking water is the optimal approach to managing this risk. The results of this study can act as a reference for the rational use of GW and for control of nitrate pollution in this area.

Keywords Groundwater quality · Nitrate pollution · Human health risk assessment · Irrigation water quality · Inner Mongolia

Introduction

Groundwater (GW) is an indispensable water resource and accounts for ~ 97% of available freshwater resources globally. Therefore, GW is very important for sustaining life, industry, and agriculture, especially in semiarid and arid areas with less rainfall and scarce surface water (Adimalla and Venkatayogi 2018; Adimalla and Wu 2019; Chen et al. 2018; Khanoranga and Khalid 2019; Wu et al. 2017; Zhang et al. 2020b; Swain et al. 2021). Unsustainable utilization of GW resources can compromise other resources (Tahmasebi et al. 2018). The quality of GW has become an increasing concern globally. There have been many studies on assessing the quality of groundwater (Adimalla et al. 2020a; Ayogu et al. 2021; Dash and Kalamdhad 2021; Qiu 2010; Raja and Neelakantan 2021; Swain et al. 2022a; Zhang et al. 2020a, 2020b). GW resources in mining areas are of particular importance for protecting the domestic water supply, supporting economic development, and maintaining the ecological balance (Chi et al. 2021; Feng et al. 2020a). Mining can result in serious consumption and pollution of GW and surface water flowing through mining areas. In addition, mining can also affect the domestic, industrial, and agricultural water use in the mining area (Chi et al. 2021; Hamdi et al. 2021; Quintanilla-Villanueva et al. 2020). There has been a gradual increase in GW exploitation in recent years due to the impact of human activities such as mining and agriculture. It has been recognized for a long time that coal mining results in environmental pollution and water quality deterioration (Feng et al. 2020a; Jebastina and Arulraj 2018; Ward et al. 2018). Therefore, identifying approaches

✉ Xueliang Zhang
zhangxueliang2021@163.com

[1] Inner Mongolia Land Resources Exploration and Development Co., Ltd, Hohhot 010020, Inner Mongolia, China

of minimizing damage to groundwater resources through the mining of coal and other anthropogenic activities is of great significance to ensure sustainable development and for achieving national energy security (Feng et al. 2020a; Luo and Wang 2019).

Agriculture is the sector that uses the most water globally (Xu et al. 2019a). Therefore, irrigation water quality and quantity have been a constant focus of policy makers and scholars. There have been many past studies on irrigation water quality globally (Feng et al. 2020b; Hosseinifard and Aminiyan 2015; Li et al. 2018). The safety of water for agricultural irrigation depends to a large degree on GW resources. Past studies have shown that under the same type of cultivated land, the economic benefit that can be achieved through irrigated grain agriculture can exceed that of rainfed grain agriculture by a factor of 2–4 (Xu et al. 2019a). The sodium absorption rate (SAR), electrical conductivity (EC), and other indicators have been widely applied within the assessment of the quality of irrigation water since these indicators make full use of the information provided by water quality variables and present the overall water quality of irrigation water through clear standard values (Kawo and Karuppannan 2018; Tahmasebi et al. 2018; Xu et al. 2019a).

Nitrate pollution is evident in shallow GW of many arid and semiarid regions (Jianyao et al. 2007; Li et al. 2016b). Nitrate is a prevalent pollutant of GW and has a significant impact GW quality. Routes of nitrate in GW into the human body include the consumption of drinking water and water contact with skin (Gao et al. 2020; Feng et al. 2020a; Zhang et al. 2019). Therefore, there is value in exploring the risk posed by nitrate pollution in drinking water to human health (Qian et al. 2020; Feng et al. 2020a; Zhang et al. 2019). The assessment of the risk posed to human health by GW links water environmental pollution with human health (Bahita et al. 2021a, 2021b; Zhang et al. 2021b, 2019; Feng et al. 2020a) and can quantitatively describe the risk to health of exposure to a polluted environment (Zhang et al. 2021a); Adimalla et al. 2020b; Zhang et al. 2019). GW pollution can affect human health (Li et al. 2016b; Zhang et al. 2019, 2021b). In particular, the consumption of water with excessive nitrate contents can lead to various health problems, including miscarriage, blue baby syndrome, methemoglobinemia and gastric cancer, gastric wall damage, oral ulcers, and reproductive damage (Paladino et al. 2018; Wu et al. 2019; Zhang et al. 2019). Therefore, the study of the risk posed by nitrate pollution to human health is of great significance.

Hydrochemical characteristics of GW are widely used to describe the source of ions, the type of GW, the interaction between GW and rock, and the GW environment (Xu et al. 2019a; Zhang et al. 2019). The determination of the hydrogeochemical characteristics and quality of GW is helpful to reveal the mechanism of interaction between GW and the environment, and can provide new insights for the conservation and management of water (Li et al. 2015; Qian et al. 2012). In addition, the identification of spatial distribution characteristics of GW hydrogeochemical parameters is very important for the judgment of groundwater flow system and the determination of groundwater pollution sources (Zhang et al. 2019). Remote sensing (RS) and geographical information systems (GIS), which are advancing expeditiously to generate rapid, continuous, and accurate results with high precision, are widely used in all fields of society and the environment (Guptha et al. 2021, 2022; Patel et al. 2022; Sahoo et al. 2021; Swain et al. 2022b, 2022c). In recent years, the use of GIS for groundwater pollution and risk assessment has also developed rapidly (Bahita et al. 2021a; Swain et al. 2022a).

The Selian mining area, Inner Mongolia, is in the center of the Ordos energy and heavy chemical industry and is an important coal production base in Ordos. However, a few studies have evaluated the quality of GW in this area. Therefore, the aims of the present study were to: (1) investigate the mechanism of formation, hydrogeochemical characteristics, and hydrochemical phases of GW in the study area; (2) evaluate the quality of irrigation water; (3) evaluate the non-carcinogenic health risk posed by nitrate-contaminated GW. The results of the present study can provide an important basis for GW quality conservation and preservation in the study area.

Study area

As shown in Fig. 1, the Selian coal mining area (109°43′09″–109°49′50 ″W, 39°52′27″–39°59′50″N) is in Ordos City, Inner Mongolia Autonomous Region. The study area falls to the north of the Ordos Plateau with an elevation of 1391.5–1504.0 m, decreasing from south to north with a relative elevation difference of ~ 40 m. Cenozoic geological forces destroyed the original geomorphic features of the plateau. The terrain of the study area is strongly cut with developed valleys, and has typical erosive hilly landform.

The Selian coal mining area falls within a monsoon, mid-temperate, semiarid, and semidesert climate zone, characterized by cold winters, a prevailing northwest wind in spring, hot summers, and cool autumns. The study area exhibits extreme temperature differences between summer and winter, and night and day, as well as low rainfall and high evaporation. The Selian coal mining area has an uneven spatial distribution of annual precipitation. Rainfall is highly seasonal, with 66% of annual rainfall falling in July, August, and September. The region experiences a long annual freezing period from October to April of the following year. No annual surface water runoff and lakes (Nurs) occur in and around the study area. Surface water from rainfall collects in

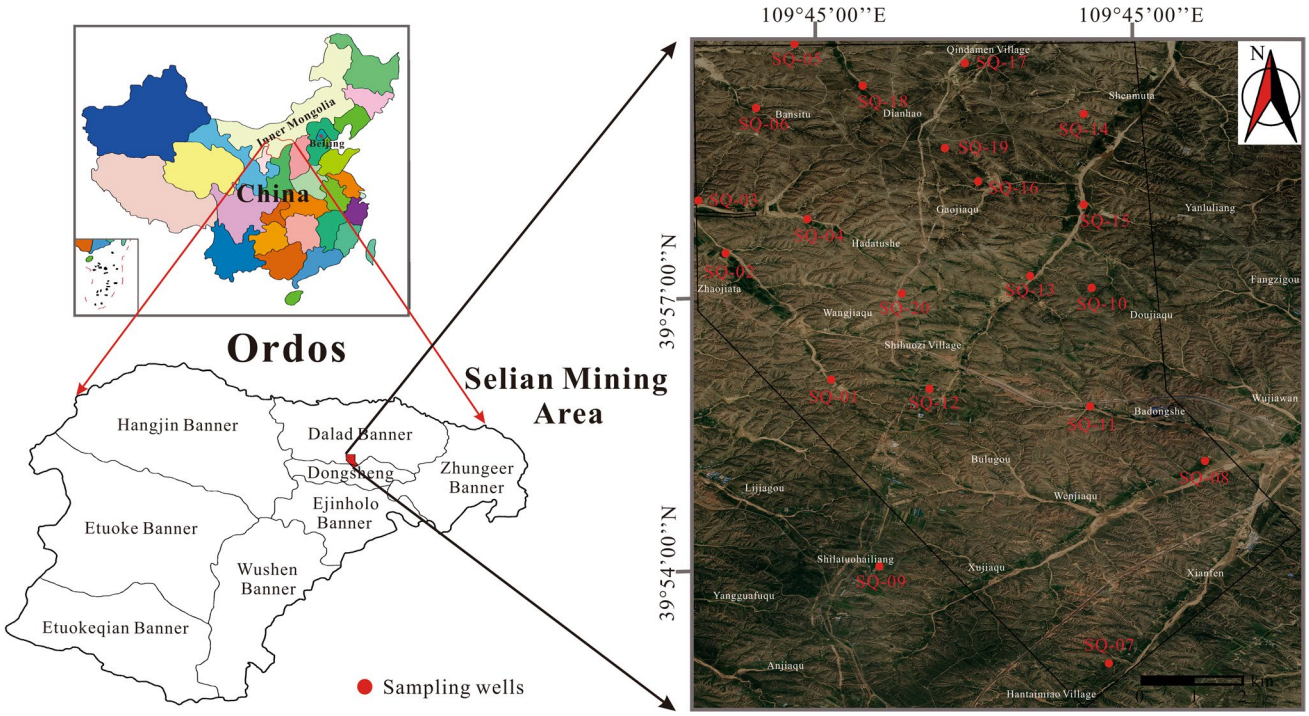

Fig. 1 Location of the study area (modified after: Feng et al. 2020a)

the tributaries of the upper reaches of the Hantaichuan River to the south of the study area during the rainy season. This water then flows into the main river channel in the study area and finally northward into the Yellow River. A short period of flow or flood occurs in the Hantaichuan River only during the rainy season, characterized by a short duration and large flow, whereas the river generally remains dry during the rest of the year.

According to hydrogeological survey, phreatic water is distributed widely in the study area. The lithology of the aquifer is mainly grayish yellow and brownish yellow alluvial proluvial sand gravel (Q_4^{al+pl}), residual slope, loess (Q_{3-4}), and aeolian sand (Q_4^{eol}). The thickness of the aquifer is 2.60–5.81 m, the elevation of the GW level is 1,297.03–1,378.38 m, the depth of GW is generally less than 10 m, and the aquifer has a moderate water yield and strong water permeability. In addition, the lower Cretaceous Zhidan group (K_{1zh}) aquifer partially merges with the upper phreatic aquifer, forming a unified aquifer rock mass. GW recharge is generally small due to low precipitation and poor supply conditions, although recharge increases significantly during the rainy season. The phreatic aquifer has a close hydraulic relationship with atmospheric precipitation and surface water, although it has a weaker relationship with the underlying confined aquifer. Phreatic water is mainly discharged by evaporation, recharge of surface water, recharge of deep confined water, and lateral runoff, followed by artificial mining.

Materials and methods

Collection and analysis of samples

The present study identified the hydrogeochemical characteristics of GW in the study area and assessed the risk of GW quality for agricultural irrigation and humane health. A sampling survey was conducted in the study area, and 20 GW samples were collected during this period. In May 2020, all samples were collected in the phreatic aquifer. Sampling was done using standard 125 mL polyethylene bottles. The sample bottles were rinsed with deionized water prior to sampling. During the collection of a water sample in the field, the sample bottle was first rinsed in triplicate using the source of the sample water, after which a sample was collected and the sample bottle sealed. The coordinates of each sample were recorded using a global positioning system (GPS). The well and GW depths of the sample well were also recorded. On-site measurements of pH, electrical conductivity (EC), and water temperature (T) were conducted. The samples were transported to a water quality analysis laboratory as soon as possible. The laboratory tests included determinations of Na^+, K^+, Cd^{2+}, Cu^{2+}, Pb^{2+}, Zn^{2+} and Mn^{2+} by flame atomic absorption spectrophotometry, Ca^{2+} and Mg^{2+} by ethylenediaminetetraacetic (EDTA) titration, $SO_4^{2-}$and Cl^- by ion chromatography, NO_3^- by ultraviolet spectrophotometry,

HCO_3^- by acid–base titration, As by atomic fluorescence spectrometry, and Cr^{6+} by Spectrophotometry.

Charge balance error (CBE) was calculated using Eq. (1) to validate the accuracy of the measurements and to estimate of the standard error of each sample (Adimalla and Qian 2021; Khanoranga and Khalid 2019; Xu et al. 2019a). CBE values within a limit of ± 5% were considered acceptable (Adimalla and Qian 2021; Xu et al. 2019a).

$$\mathrm{CBE} = \frac{\sum cations - \sum anions}{\sum cations + \sum anions} \times 100\%. \quad (1)$$

The concentrations of cations and anions were expressed in meq/L. The results indicated that the CBE values of all water samples ranged from − 2.73 to 2.69, thereby corroborating the reliability of the analysis.

Mineral saturation indices

At present, the saturation indices method is the most used method to judge and describe the saturation state of minerals relative to groundwater. Saturation indices (SI) are the most widely used index in groundwater hydrochemistry. When SI = 0, it indicates that the mineral and water reach the dissolution equilibrium state; When SI < 0, it indicates that the mineral and water are in unsaturated state, and the mineral has the trend of continuous dissolution in water; When SI > 0, it indicates that the mineral is in a supersaturated state and tends to precipitate from water (Xu et al. 2021b).

$$SI = \lg \frac{IAP}{K} \quad (2)$$

where *IAP* is the ion activity product; *K* is the equilibrium constant for a mineral at a given temperature.

Correlation analysis

Correlation analysis is a statistical method to study the relationship between variables (Zhang et al. 2021c). It is used to explore the correlation degree of dependent variables, and reveal the similarity and difference of sources among various variables (Zhang et al. 2021b). The correlation coefficient is calculated by the following formula:

$$rij = \frac{\sum_{i=1}^{n} (xi - \bar{x}) \sum_{j=1}^{n} (yj - \bar{y})}{\sqrt{\sum_{i=1}^{n} (xi - \bar{x})^2 \sum_{j=1}^{n} (yj - \bar{y})^2}} \quad (3)$$

where r_{ij} is the correlation coefficient between variable *i* and variable *j*, x_i is the value of the *i*-th variable, y_j is the value of the *j*-th variable, $\bar{x}$ is the average value of the *i*-th variable, $\bar{y}$ is the average value of the *j*-th variable, *i* and *j* are selected water sample index, *n* is the total number of water samples.

Evaluation of GW quality for agricultural irrigation

GW is widely utilized for agricultural irrigation in the study area. Irrigation water quality reflects its mineral composition and the effect of irrigation on soil and plants (Khanoranga and Khalid 2019; Xu et al. 2019a), and high concentrations of salts in irrigation water can lower agricultural productivity (Khanoranga and Khalid 2019; Xu et al. 2019a). Therefore, the assessment of agricultural irrigation water quality is important to optimize agricultural production in the study area. The current study used the percentage sodium (Na%), sodium absorption ratio (SAR), comprehensive hazard coefficient (K), and Irrigation coefficient (K_a) parameters to assess the quality of irrigation water (Adimalla and Qian 2021; Li et al. 2016b; Xu et al. 2019a):

$$\mathrm{Na\%} = \frac{\left(Na^+ + K^+\right) \times 100}{Ca^{2+} + Mg^{2+} + Na^+ + K^+} \quad (4)$$

$$\mathrm{SAR} = \frac{Na^+}{\sqrt{\left(Ca^{2+} + Mg^{2+}\right)/2}} \quad (5)$$

$$\mathrm{K} = 12.4M + SAR \quad (6)$$

$$\mathrm{K}_a = \begin{cases} \frac{288}{5Cl^-} & if\ Na^+ < Cl^- \\ \frac{288}{Na^+ + 4Cl^-} & if\ Cl^- < Na^+ < Cl^- + 2SO_4^{2-} \\ \frac{288}{10Na^+ - 5Cl^- - 9SO_4^{2-}} & if\ Na^+ > Cl^- + 2SO_4^{2-} \end{cases} \quad (7)$$

where M is total dissolved solids (g/L), and the concentrations of all ions were expressed in meq/L.

Evaluation of GW quality for risk posed to human health

The presence of nitrate in drinking water poses a serious risk to human health through two main exposure routes (Adimalla and Qian 2021): (1) consumption of drinking water; (2) skin contact. The integrated human health risk assessment model was first proposed by the United States of America Environmental Protection Agency (US EPA) (2012). The present study considered both the skin and oral exposure pathways. The population that depends on GW can be divided into two categories according to differences in physiology and behavior: (1) children (< 17 years old); (2) adults (> 18 years old). The present study evaluated non-carcinogenic risk based on the potential pollutant (NO_3^-) in GW.

The non-carcinogenic risk of GW skin exposure can be determined as follows (Manassaram et al. 2010; WHO 2011):

$$CDI_{dermal} = (C_i \times K \times S_a \times T \times EF \times ED \times EV \times CF)/(BW \times AT) \quad (8)$$

$$S_a = 239 \times BH^{0.417} \times BW^{0.517} \quad (9)$$

$$HQ_{dermal} = CDI_{dermal}/RfD_{dermal} \quad (10)$$

$$RfD_{dermal} = RfD_{oral}/ABS_{gi}. \quad (11)$$

In Eq. (8), CDI_{dermal} is the daily exposure dose received through the consumption of drinking water [mg/ (kg × day)], T is the hourly contact duration (h/d), ED is the yearly contact duration (years), AT is the average daily contact duration (days, AT = ED × 365), EV is the hourly frequency of skin contact (hours/day), EF is the daily frequency of exposure (days/year), CF is the unit conversion factor (L/cm^3), C_i is the target pollutant concentration in GW (mg/L), K is the skin permeability parameter (cm/h), and BW was the average body weight (kg). In Eq. (9), S_a is the skin surface area and BH is the average height (cm). In Eq. (10), RfD_{dermal} is the reference dose of the pollutant [mg/(kg × day)] through the skin contact route and HQ_{dermal} is the non-carcinogenic risk posed by the pollutant through skin contact. In Eq. (11), ABS_{gi} is the gastrointestinal absorption factor.

The non-carcinogenic risk posed by a pollutant through the oral route can be assessed as follows:

$$CDI_{oral} = (C_i \times IR \times EF \times ED)/(BW \times AT) \quad (12)$$

$$HQ_{oral} = CDI/RfD_{oral}. \quad (13)$$

In Eq. (12) and Eq. (13), CDI_{oral} is the chronic daily intake dose [mg/(kg × day)] through the consumption of drinking water, HQ_{oral} is the non-carcinogenic risk through consumption of drinking water, IR is the rate of consumption of drinking water (L/day), and RfD_{oral} is the reference dose of the pollutant through drinking water [mg/(kg × day)]. The USEPA (USEPA, 2012) nitrate limit is 1.6 mg/kg/day. Table 1 lists the values of the parameters for the health risk assessment calculated in the present study.

The total non-carcinogenic risk ($HQ_{total,I}$) of a specific pollutant through both skin contact and consumption of drinking water is as follows:

$$HQ_{total,I} = HQ_{oral,i} + HQ_{dermal,i}. \quad (14)$$

Results and discussion

Groundwater chemistry

Table 2 describes the chemical properties of the GW samples. The GW in the phreatic aquifer was found to be alkaline with a low variation. The total dissolved solids of the GW ranged between 365.60 and 922.91 mg/L; however, TDS did not exceed 1,000 mg/L, showing that GW in this area is suitable for drinking water. The order of the main ions found in GW in the study area according to concentration was: $Ca^{2+} > Na^+ > Mg^{2+} > K^+$. Total hardness (TH) of the GW ranged between 205.17 and 570.48 mg/L, with $CaCO_3$ contributing most to hardness. GW with high concentrations of Ca^{2+} and Mg^{2+} usually exhibits higher water hardness. The presence of $Ca^{2+}$and Mg^{2+}in GW can be attributed to the dissolution of minerals such as carbonate and gypsum. The rank of the main anions in GW according to concentration was: $HCO_3^- > SO_4^{2-} > Cl^- > NO_3^-$. Trace elements such as Cd^{2+}, Cu^{2+}, Pb^{2+}, Zn^{2+}, Mn^{2+}, Cr^{6+}, and As in the study area are lower than the lower limit of detection, and As is 0.002 mg/L only in SQ-10. Therefore, these trace elements will not be further studied.

As shown in Fig. 2, the spatial distribution characteristics of Mg^{2+}, Ca^{2+}, and SO_4^{2-} in the study area are similar, their content is generally high in the north and south sides and low in the middle, suggesting that they may have the same source. The distribution of Cl^- is similar to that of Na^+ and K^+, which is lower in the north and higher in the south, indicating there are similar hydrogeochemical processes in the water–rock interaction system. NO_3^- (Fig. 2f) is high in the north and low in the south, which is opposite to the distribution of HCO_3^- (Fig. 2h).

Hydrochemical facies

The plotting of the main GW chemical compositions in a Piper diagram can assist in GW quality classification (Adimalla and Qian 2021; Li et al. 2016b; Xu et al. 2019a, 2019b, 2019c). Hydrochemical facies represent zones describing the dominant cations and anions affecting GW hydrochemistry (Adimalla and Qian 2021; Xu et al. 2019a). As shown in Fig. 3, cations of GW samples collected in the study region mainly were

Table 1 Exposure parameters of human health risk assessment in different groups

Exposure Parameter	EF(days/year)	ED(years)	IR(L/day)	BW(kg)	BH(cm)	T(h/d)	ABS_{gi}	EV(day)	CF(L/cm^3)	K(cm/h)
Children	365	6	1.5	25.9	117	0.4	0.5	1	0.002	0.001
Adult	365	30	3.62	73	165.3	0.4	0.5	1	0.002	0.001

Table 2 Physicochemical groundwater characteristics

Index	pH	TH (mg/l)	TDS (mg/l)	Ca^{2+} (mg/l)	Mg^{2+} (mg/l)	K^{+} (mg/l)	Na^{+} (mg/l)	Cl^{-} (mg/l)	HCO_3^{-} (mg/l)	SO_4^{2-} (mg/l)	NO_3^{-} (mg/l)
Max	8.48	570.48	922.91	118.24	71.70	4.30	163.01	177.27	524.67	288.00	109.57
Min	7.80	205.17	365.60	42.08	24.31	0.39	32.65	35.45	183.02	57.60	0.80
Mean	8.11	421.85	678.11	78.06	55.11	1.15	77.71	81.72	330.36	186.00	23.57
Median	8.06	420.42	666.11	82.16	55.90	0.78	65.52	67.36	305.04	177.60	16.99

plotted in zone B, indicating there is no cation-dominated type in GW. Anions are mainly plotted in zone B followed by E, indicating that groundwater could be divided into two groups, in which no anion is dominant in the first group and in which bicarbonate is dominant in the second group. Almost all GW samples are plotted in zones 5 and 1, followed by zones 2 and 3, illustrating that the dominant GW types are mixed and Ca–HCO_3, followed by Na–Cl and Ca–Cl. The hydrochemical types identified could mainly be related to dissolution of minerals and salts within the aquifers.

Natural mechanisms driving groundwater quality

An improved understanding of the factors driving GW chemistry is important for the protection of GW quality and for the development of GW resources (Xu et al. 2021a, 2019a). Gibbs diagrams (Fig. 4) were proposed by Gibbs (1970) for studying the mechanisms driving the chemical compositions of water. A Gibbs diagram consists of two sub-diagrams. The first represents the relationship between TDS and the weight ratio of Na^+ versus ($Na^+ + Ca^{2+}$). The second represents the relationship between TDS and the weight ratio of Cl^- versus ($Cl^- + HCO_3^-$) (Li et al. 2016a). The Gibbs diagram represents three processes driving the chemical composition of GW (Li et al. 2016a; Zhang et al. 2020b): (1) Rock Dominance; (2) Evaporation Dominance, and; (3) Precipitation Dominance.

As shown in Fig. 4, almost all GW samples are shown to fall within the rock dominance category, suggesting that the weathering of rock and leaching are the primary mechanisms driving GW chemistry in the study area. Large quantities of dissolvable salts and minerals are found in sediments as the sediments are produced by the weathering of parent rock. These soluble salts enter GW through soil infiltration of irrigation water and precipitation.

Sources of major ions

The Gibbs diagrams showed that GW quality in the study area fell within a rock dominance category. The bivariate diagram of ions shown in Fig. 5 further supported the above result. The Na^+ versus Cl^- plot indicated a clear Na^+ enrichment in the GW samples (Fig. 5a). The GW ratios of Na^+/Cl^- in the study area ranged from 0.63 to 2.53 with an average of 1.58. Generally, under a situation of halite dissolution being the sole source of GW quality, the Na^+/Cl^- ratio should approximate 1 (Li et al. 2016a; Xu et al. 2021b; Zhang et al. 2020b). Most of the samples showed higher Na^+/Cl^- ratios, thereby suggesting an additional source of Na^+. The weathering of silicate may occur under an alkaline environment [Eq. (15) and Eq. (16)]. Processes of cation exchange may also result in high concentrations of Na^+ in GW.

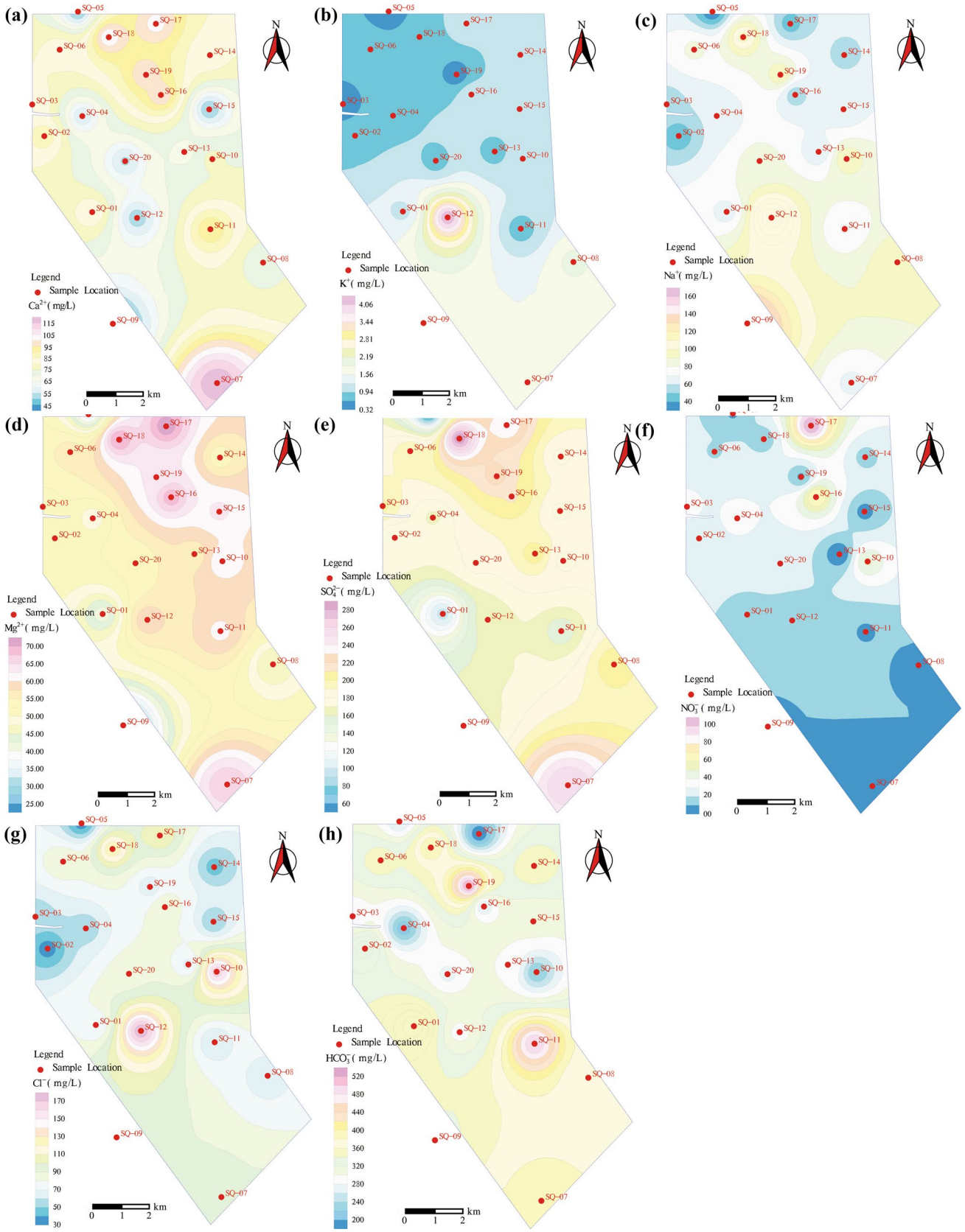

Fig. 2 Spatial distribution map of main ions: (a) Ca^{2+}, (b) K^{+}, (c) Na^{+}, (d) Mg^{2+}, (e) $SO_4{}^{2-}$, (f) $NO_3{}^{-}$, (g) Cl^{-}, and (h) $HCO_3{}^{-}$

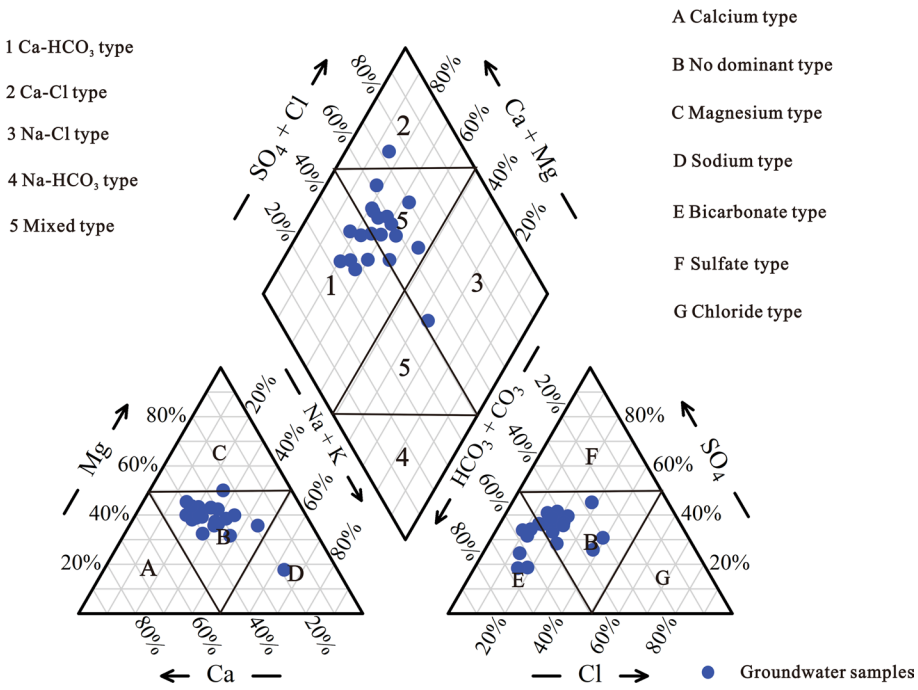

Fig. 3 Piper diagram for groundwater samples

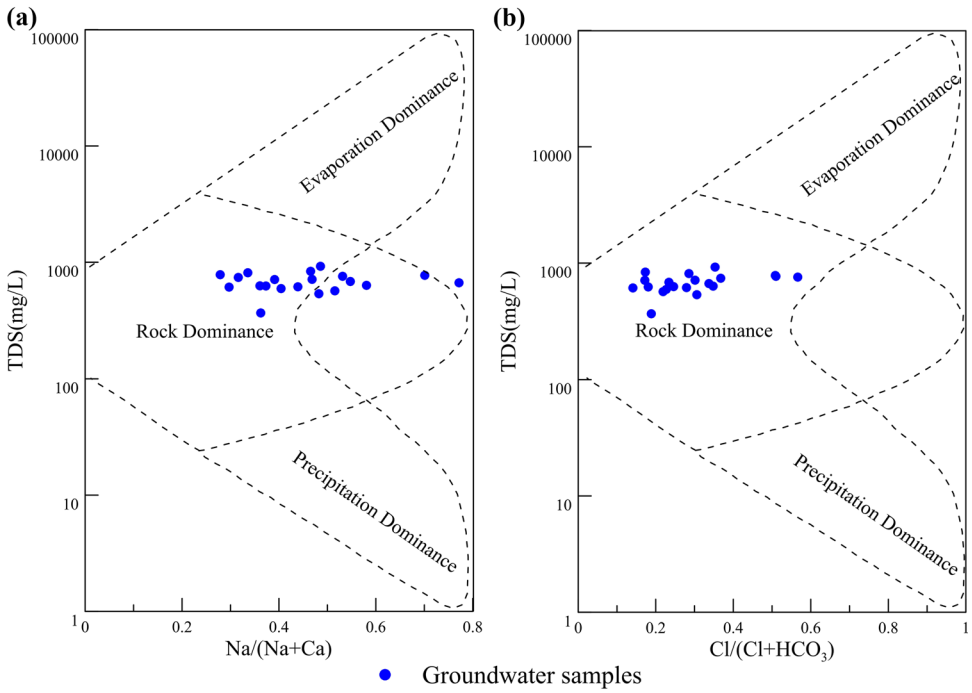

Fig. 4 Gibbs diagrams of groundwater samples

$$3Na_{1/3}Al_{7/3}Si_{11/3}O_{10}(OH)_2 + 30H_2O + 6OH^- \rightarrow Na^+ + 7Al(OH)_4^- + 11H_2SiO_4 \quad (15)$$

$$4NaAlSi_3O_8 + 4CO_2 + 22H_2O \rightarrow 4Na^+ + 4HCO_3^- + Al_4(Si_4O_{10})(OH)_8 + 8H_4SiO_4. \quad (16)$$

The ratio of $HCO_3^- + SO_4^{2-}$ to $Ca^{2+} + Mg^{2+}$ in GW would approximate 1 if the dissolution of carbonates and sulfate minerals is the main process affecting GW chemistry (Li et al. 2016b; Zhang et al. 2020b). As shown in Fig. 5b, almost all GW samples collected in the study area are plotted above the 1:1 line. The fact that $HCO_3^- + SO_4^{2-}$ was dominant over $Ca^{2+} + Mg^{2+}$ in the GW samples may be due to the weathering of carbonates

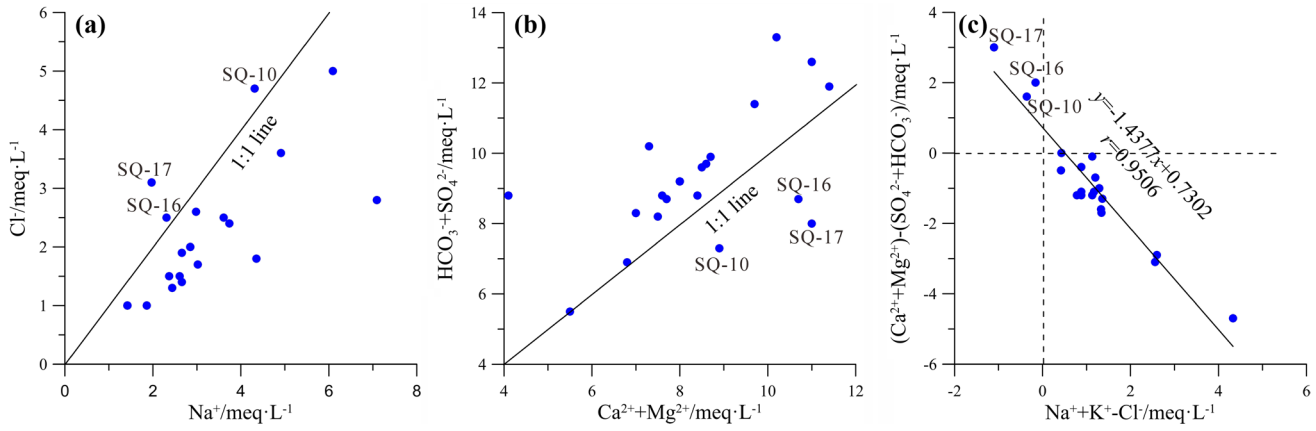

Fig. 5 Bivariate diagrams of major ionic concentrations in groundwater samples

and sulfate minerals as well as cation exchange. However, a few samples (SQ-10, SQ-16, and SQ-17) are plotted under the 1:1 line, showing that GW in this area undergoes reverse cation exchange. The ratio of Na^+/Cl^- further supported this assertion. The linear relationship between $Na^+ + K^+$-Cl^- and $(Ca^{2+} + Mg^{2+})$-$(HCO_3^- + SO_4^{2-})$ similarly had a slope of − 1 under the condition of cation exchange being the primary processes affecting the chemical composition of GW (Adimalla and Qian 2021; Xu et al. 2021b). As shown in Fig. 5c, the slope of the linear regression line was − 1.4377, diverging slightly from − 1. This result indicated that cation exchange and reverse cation exchange occur in the GW system, although these processes have little influence on GW quality in the study area.

The main mineral saturation indexes in groundwater samples were calculated and are shown in Table 3. The saturation index of gypsum and halite in groundwater was negative and in unsaturated state. This indicated that gypsum and halite have a dissolution trend, which was consistent with the above results. The saturation index of calcite and dolomite was positive with a precipitation tendency. However, the results of bivariate diagrams of major ionic concentrations show that a source of Ca^{2+} and Mg^{2+} was the dissolution of carbonate minerals. In fact, they were not contradictory. The dissolution of calcite and dolomite existed in the groundwater environmental system, while it was in a saturated state.

Analysis of the correlations between ions in GW

The geochemical processes driving the chemical compositions of GW in an aquifer can be identified through the assessment of the correlations between the various chemical constituents of GW samples (Xu et al. 2019c; Zhang et al. 2020b).

Table 3 Calculation for mineral saturation index

Sample no	Gypsum	Halite	Calcite	Dolomite
SQ-01	− 1.68	− 6.92	1.06	2.15
SQ-02	− 1.43	− 7.41	1.05	2.21
SQ-03	− 1.38	− 7.13	0.95	2.04
SQ-04	− 1.6	− 7.08	1.02	2.33
SQ-05	− 2.04	− 7.51	0.98	2.18
SQ-06	− 1.42	− 6.73	1.03	2.24
SQ-07	− 1.19	− 6.80	1.02	2.14
SQ-08	− 1.43	− 6.79	0.82	1.78
SQ-09	− 1.73	− 6.38	0.94	1.98
SQ-10	− 1.50	− 6.38	1.05	2.35
SQ-11	− 1.49	− 6.98	1.28	2.72
SQ-12	− 1.69	− 6.20	0.69	1.78
SQ-13	− 1.46	− 6.98	0.96	2.18
SQ-14	− 1.45	− 7.18	0.94	2.04
SQ-15	− 1.65	− 7.11	1.06	2.58
SQ-16	− 1.33	− 6.93	0.85	1.88
SQ-17	− 1.28	− 6.91	0.79	1.76
SQ-18	− 1.22	− 6.45	1.29	2.75
SQ-19	− 1.32	− 6.8	0.97	2.09
SQ-20	− 1.59	− 6.73	0.55	1.44

As shown in Table 4, the concentrations of major ions in the GW samples were positively correlated with TDS, which could be attributed to the long residency of GW in the aquifer, thereby increasing aquifer water–rock interactions. A significant positive correlation was identified between the concentrations of Na^+ and Cl^-, and SO_4^{2-} was also positively correlated with both Ca^{2+} and Mg^{2+}. These results indicated the main sources of these ions to be the dissolution of rock salt, gypsum, dolomite, and calcite. In addition, since the correlation between Ca^{2+} and SO_4^{2-} exceeded that

Table 4 Correlation matrix of the physicochemical water parameters

Catalog	PH	TDS	K^+	Na^+	Ca^{2+}	Mg^{2+}	Cl^-	SO_4^{2-}	HCO_3^-	NO_3^-
PH	1	− 0.386	− 0.154	− 0.006	− .489*	− 0.215	0.027	− 0.29	− 0.43	0
TDS		1	0.255	0.479*	0.638**	0.652**	0.632**	0.803**	0.326	0.187
K^+			1	0.541*	− 0.241	0.033	0.616**	− 0.007	− 0.113	− 0.069
Na^+				1	− 0.278	− 0.2	0.631**	0.17	0.203	− 0.307
Ca^{2+}					1	0.649**	0.037	0.605**	0.405	0.289
Mg^{2+}						1	0.34	0.686**	0.022	0.41
Cl^-							1	0.296	− 0.234	0.269
SO_4^{2-}								1	0.1	0.205
HCO_3^-									1	− 0.598**
NO_3^-										1

between Ca^{2+} and HCO_3^-, dissolution of gypsum may be the main source of Ca^{2+}.

Na^+ was negatively correlated with Ca^{2+} and Mg^{2+}, indicating that the dissolution of gypsum, anhydrite, and calcite provides sufficient Ca^{2+} and Mg^{2+} and promotes cation exchange. There was a significant positive correlation between Mg^{2+} and SO_4^{2-}, which could be attributed to dolomite dissolution and dolomitization.

The suitability of groundwater for irrigation

The assessment of water quality is important within agricultural irrigation. The present study evaluated the suitability of GW in the study area for agricultural irrigation through the use of the single indices (%Na, SAR), K, and K_a. Table 5 shows a summary of the values of these indices within the GW of the study area.

SAR and %Na are commonly used to quantify the potential sodium hazard of irrigation water. As per SAR, GW with SAR < 10, 10 < SAR < 18, 18 < SAR < 26, and SAR > 26 is classified as being of excellent, good, acceptable, and unacceptable quality for use in agricultural irrigation (Krishnakumar et al. 2014; Ravikumar et al. 2013). GW with %Na < 30%, 30% < %Na < 60%, and %Na > 60% is classified as suitable, marginally suitable, and unsuitable for agricultural irrigation, respectively (Li et al. 2016a; Ravikumar et al. 2013; Vasanthavigar et al. 2012). As shown in Table 5, the SAR of GW in the study area ranged between 0.84 and 4.95 with a mean of 1.72 and a median of 1.37, indicating that GW was suitable for agricultural irrigation. The %Na of GW ranged between 15.39% and 63.49% with an average of 28.61% and a median of 25.89%, suggesting that the majority of GW in the study area was suitable for irrigation, some water was marginally suitable, and only one water sample was found to be unsuitable for agricultural irrigation.

Electrical conductivity (EC) of agricultural irrigation water is a measure of the salinity hazard posed by irrigation water to crops. Salts contained in irrigation water can directly affect plant growth, and these salts also indirectly affect plant growth by influencing soil structure permeability and aeration (Adimalla and Qian 2021). GW with low and moderate salinities of less than 250 µS/cm and between 250 and 750 µS/cm can be classified as excellent and suitable for agricultural irrigation, respectively, whereas GW with an EC in the range of 750–2,250 µS/cm was unsuitable for agricultural irrigation and should be used with caution. The use of GW with an EC exceeding 2,250 µS/cm for agricultural irrigation will result in soil salinization and reduce crop productivity. In the present study, the EC of all water samples ranged between 750 and 2,250 µS/cm, indicating that

Table 5 Indicators for irrigation water quality assessment

Sample no.	EC(µS/cm)	%Na	SAR	K	K_a
SQ-01	1186.26	27.48	1.46	8.82	26.54
SQ-02	1221.81	17.94	0.90	8.47	49.14
SQ-03	1252.79	22.08	1.16	8.92	34.41
SQ-04	1069.82	27.89	1.42	8.05	33.45
SQ-05	731.20	20.64	0.86	5.39	53.13
SQ-06	1423.61	29.44	1.73	10.56	21.16
SQ-07	1627.05	20.95	1.25	11.34	21.52
SQ-08	1367.88	37.61	2.28	10.76	24.93
SQ-09	1332.22	63.49	4.95	13.21	15.75
SQ-10	1514.41	32.78	2.04	11.43	12.25
SQ-11	1417.39	23.86	1.37	10.16	33.88
SQ-12	1539.55	45.26	3.15	12.69	11.52
SQ-13	1231.35	25.10	1.33	8.96	30.31
SQ-14	1246.59	22.52	1.18	8.91	44.30
SQ-15	1136.51	25.89	1.36	8.40	41.14
SQ-16	1479.00	17.95	1.00	10.17	23.04
SQ-17	1564.17	15.39	0.84	10.54	18.58
SQ-18	1845.82	30.95	2.09	13.54	16.00
SQ-19	1670.99	29.95	1.93	12.29	32.00
SQ-20	1266.12	34.95	2.00	9.85	24.00
Mean	1356.23	28.61	1.72	10.12	28.35
Median	1332.22	25.89	1.37	10.16	24.93

although GW in the study area was acceptable for irrigation, it should be used with caution.

The US Salinity Laboratory (USSL) and Wilcox diagrams provide a simple method of relating salinity and alkalinity for the assessment of irrigation water quality; therefore, these diagrams are widely used in research (Li et al. 2016a). In this study, these two diagrams of GW samples were drawn using Grapher 10, with the help of references of Xu et al. (2019a) and Li et al. (2016a). As shown in Fig. 6, all water samples are plotted in zone C3S1, indicating that the GW of the study area was of high and low salinity and alkalinity, respectively; thus, although GW of the study area was acceptable for agricultural irrigation, it should be used with caution.

A Wilcox diagram was used to assess the suitability of GW for irrigation (Li et al. 2016a). As shown in Fig. 7, most of the GW samples were categorized as being of good quality or acceptable for agricultural irrigation, although the GW should be used with caution. The suitability of two GW samples for irrigation was identified to range between permissible to doubtful, suggesting poor suitability of GW in the study area for irrigation.

The K composition of water can reflect the salt and alkali hazard posed by that water. GW with $K < 25$, $25 < K < 36$, $36 < K < 44$, and $K > 44$ is classified as of excellent, good, moderately unsuitable, and unsuitable for agricultural irrigation, respectively (Xu et al. 2019a). As shown in Table 5, the K values of the GW samples ranged from 5.39 to 13.54 with a mean of 10.12 and a median of 10.16; therefore, all GW samples were classified as having

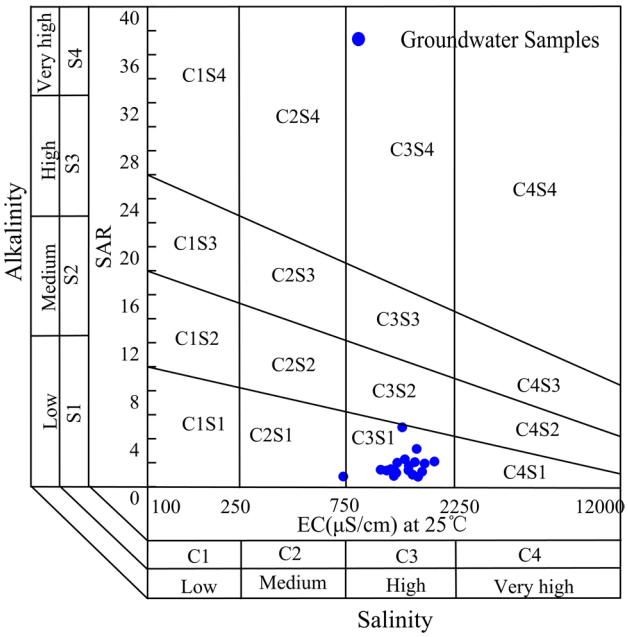

Fig. 6 USSL diagram for irrigation water quality assessment

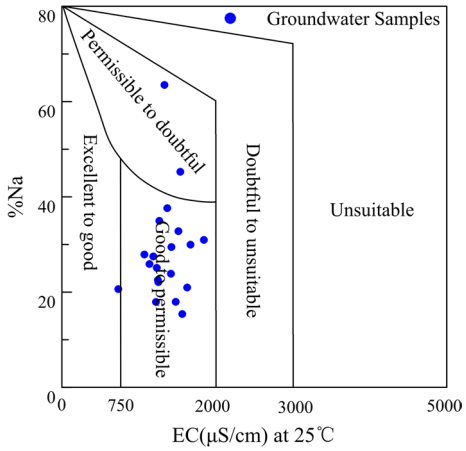

Fig. 7 Wilcox diagram for irrigation water quality assessment

excellent quality for agricultural irrigation. The quality of GW in the study area for agricultural irrigation was further confirmed by the fact that this evaluation method provides conservative results.

The K_a value is based on the harm caused to 40 types of crops by sodium salt relative to the greatest harm resulting from exposure to an alkaline solution. GW with $K_a > 18$, $6 < K_a < 18$, $1.2 < K_a < 6$, and $K_a < 1.2$ is classified as excellent, permissible, moderately unsuitable, and unsuitable for use in agricultural irrigation, respectively (Xu et al. 2019a). Among the GW samples, 80% and 20% were classified as excellent and permissible, respectively, indicating that GW in the study area can be used for agricultural irrigation.

The irrigation quality of groundwater in the study area is evaluated by using multiple indicators. Considering these indicators, there is no sodium hazard in groundwater irrigation, but the quality could be affected by high salinity. The reason for the high salinity of groundwater is that the study area is located in the regional watershed, and its recharge source is mainly atmospheric precipitation. However, the vegetation in the study area is scarce, the precipitation is small, the recharge is poor. In addition, the climate is arid with strong evaporation, and the groundwater discharge mode is mainly evaporation, which leads to increase in the salinity of groundwater. Therefore, when using groundwater to irrigate farmland, measures should be taken to control the salt content in the water and prevent salt accumulation in soil.

Assessment of the risk posed by GW to human health

The non-carcinogenic risk posed by GW in the study area to adults and children through different exposure routes was evaluated according to the definition of the risk index

by the US EPA (2012). As shown in Table 6, the average health risk index of children who ingested nitrate through drinking water was 0.8533, exceeding that of adults by a factor of ~ 1.168. The health risk indices for children and adults ranged between 0.02895–3.9660 and 0.02479–3.3958, respectively. The percentages of water samples with a health risk index to children and adults ranging between 0.75 and 1 were 10% and 5%, respectively. However, it was likely that the health risk index of GW in the study area exceeded 1 due agricultural activities or unsustainable exploitation, thereby posing a risk to human health. Therefore, the potential risk to human health posed by GW in the study area requires consideration. About 25% of the GW samples showed a health risk index to children and adults exceeding 1. These results indicated that the risk posed by some GW in the study area to human health was unacceptable; therefore, there should be careful monitoring of the risk posed by GW to the health of children.

The average non-carcinogenic risk posed by nitrate to children through skin contact was 0.0021, exceeding that of adults by a factor of 1.428. The non-carcinogenic risks posed by nitrate to children and adults were 7.23165×10^{-5}–0.0099 and 5.636×10^{-5}–0.006935, respectively. The non-carcinogenic risk posed by nitrate through skin contact was far less than 1, indicating that the risk posed by nitrate to health through this route is minor. The non-carcinogenic risks posed by nitrate to children through the consumption of drinking water and skin contact exceeded those of adults by factors of 1.168 and 1.428, respectively. This result can be attributed to health of children being more sensitive to exposure to environmental pollution per unit weight as compared to adults (Adimalla and Qian 2021; Ezekwe et al. 2012). Therefore, there should be increased focus on mitigating the risk posed by nitrate in the GW of the study area to the health of children.

The average total health risk index for nitrate exposure by children was 0.8554, exceeding that of adults by a factor of 1.168. The total health risk index values for children and adults ranged between 0.0290–3.9759 and 0.02484–3.4027, respectively. Approximately 20% of the samples showed a total health risk index for children and adults exceeding 1, thereby posing a risk to human health. It was evident that the majority of risk to human health posed by nitrate in GW was through the consumption of drinking water rather than skin contact, with the former accounting for 99.75% of the total risk. Therefore, it was recommended that water treatment was the most effective approach to managing the risk posed by nitrate in GW to human health in the study area.

The results of human health risk assessment show that groundwater in the study area mainly poses risks to humans through drinking water, and the risk to children is higher than that to adults. The intensity and scope of nitrate pollution show significant characteristics of human activities. For instance, SQ-17 with the highest nitrate content is located in Qingdamen village (Figs. 1 and 2f), which is the largest agricultural village in the study area. Therefore, human agricultural activities are the main source of nitrate in groundwater. After nitrogen fertilizer is applied to farmland, nitrogen not absorbed by plants enters shallow groundwater through leaching and infiltration. In addition, the excessive exploitation of groundwater leads to the decline of water level, which intensifies the dissolution of residual nitrogen in soil during groundwater recharge. This also leads to the increase in nitrate content in groundwater. In general, the south of the study area is the recharge area of groundwater, with low nitrate content, while the north of the discharge area suffered long-term evaporation and leaching has high nitrate content. Therefore, targeted measures should be taken, such as changing irrigation methods, controlling fertilizer consumption, to reduce nitrate pollution in groundwater and the risk of nitrate to human health.

Conclusions

The present study analyzed the chemical compositions of 20 shallow GW samples collected from the Selian coal mine area, Ordos, Inner Mongolia. The hydrochemical phases and main sources of ions in the GW were analyzed through correlation analysis and Piper, Gibbs, and bivariant diagrams of major ions. The quality of irrigation water was evaluated according to the irrigation water quality indices, including the sodium absorption rate, sodium percentage, K, and K_a. The risk posed by the nitrate content of GW in the study area to human health was evaluated. The main conclusions of the present study were as follows.

The main hydrochemical type of GW in the study area was mixed and Ca–HCO_3, and rock weathering and leaching were identified as the main processes driving the chemical composition of GW in the study area. The values of water

Table 6 Non-carcinogenic risk of nitrate for children and adults in drinking water and dermal contact pathway

Non-Carcinogenic	Water Intake Risk Index		Skin Contact Risk Index		Total Risk of Two Exposure Routes	
	Range	Average	Range	Average	Range	Average
Children	0.02895–3.9660	0.8533	7.23*10–^{5}-0.0099	0.0021	0.0290–3.9759	0.8554
Adult	0.02479–3.3958	0.7300	5.063*10^{-5}-0.0069	0.0014	0.02484–3.4027	0.7321

quality indices for irrigation, such as the sodium absorption rate and sodium percentage, indicate although GW in this area was suitable for irrigation, it should be used cautiously. According to the human health risk assessment model, the risks posed by nitrate in GW of the study area to the health of children through consumption of drinking water and skin contact exceeded those of adults by as much as a factor of 1.168. Drinking water was the main way for people to contact nitrate in GW. Therefore, the most effective way to reduce the risk of nitrate to human health is centralized water supply.

Acknowledgements This study was supported by the project of Detailed survey of coal in bayintaolegai exploration area, tarang-gaole mining area, Dongsheng coalfield, Inner Mongolia Autonomous Region (Project No. 20-1-MT05) by Inner Mongolia land resources exploration and Development Co., Ltd.

Declarations

Conflict of interest The authors declare that they have no known competing financial interests or personal relationships that could have appeared to influence the work reported in this paper.

References

Adimalla N, Qian H (2021) Groundwater chemistry, distribution and potential health risk appraisal of nitrate enriched groundwater: a case study from the semi-urban region of South India. Ecotoxicol Environ Safety 207:111277. https://doi.org/10.1016/j.ecoenv.2020.111277

Adimalla N, Venkatayogi S (2018) Geochemical characterization and evaluation of groundwater suitability for domestic and agricultural utility in semi-arid region of Basara, Telangana State South India. Appl Water Sci 8(1):14. https://doi.org/10.1007/s13201-018-0682-1

Adimalla N, Wu JH (2019) Groundwater quality and associated health risks in a semi-arid region of south India: implication to sustainable groundwater management. Hum Ecol Risk Assess 25(1–2):191–216. https://doi.org/10.1080/10807039.2018.1546550

Adimalla N, Chen J, Qian H (2020a) Spatial characteristics of heavy metal contamination and potential human health risk assessment of urban soils: A case study from an urban region of South India. Ecotoxicol Environ Safety 194:110406. https://doi.org/10.1016/j.ecoenv.2020a.110406

Adimalla N, Marsetty SK, Xu PP (2020b) Assessing groundwater quality and health risks of fluoride pollution in the Shasler Vagu (SV) watershed of Nalgonda India. Hum Ecol Risk Assess 26(6):1569–1588. https://doi.org/10.1080/10807039.2019.1594154

Ayogu NO, Mamah LI, Ayogu CN, Maduka RI (2021) Assessment of groundwater quality using geoelectrical potential and hydrogeochemical analysis in Eha-Amufu and environs Enugu state Nigeria. Environ Dev Sustain. https://doi.org/10.1007/s10668-020-01103-3

Bahita TA, Swain S, Dayal D, Jha PK, Pandey A (2021a) Water quality assessment of upper Ganga canal for human drinking. In: Ashish Pandey SK, Mishra ML, Kansal RD, Singh VPS (eds) Climate impacts on water resources in India: Environment and Health. Springer International Publishing, Cham, pp 371–392. https://doi.org/10.1007/978-3-030-51427-3_28

Bahita TA, Swain S, Pandey P, Pandey A (2021b) Assessment of heavy metal contamination in livestock drinking water of Upper Ganga Canal (Roorkee City, India). Arab J Geosci 14:2861. https://doi.org/10.1007/s12517-021-08874-7

Chen J, Wu H, Qian H, Li XY (2018) Challenges and prospects of sustainable groundwater management in an agricultural plain along the Silk Road Economic Belt, north-west China. Int J Water Resour Dev 34(3):354–368. https://doi.org/10.1080/07900627.2016.1238348

Chi M, Zhang D, Zhao Q, Yu W, Liang S (2021) Determining the scale of coal mining in an ecologically fragile mining area under the constraint of water resources carrying capacity. J Environ Manag 279:111621. https://doi.org/10.1016/j.jenvman.2020.111621

Dash S, Kalamdhad AS (2021) Hydrochemical dynamics of water quality for irrigation use and introducing a new water quality index incorporating multivariate statistics. Environ Earth Sci. https://doi.org/10.1007/s12665-020-09360-1

US EPA. (2012). 2012 Edition of the drinking water standards and health advisories. EPA 822-S-12–001

Ezekwe IC, Odu NN, Chima GN, Opigo A (2012) Assessing regional groundwater quality and its health implications in the Lokpaukwu, Lekwesi and Ishiagu mining areas of southeastern Nigeria using factor analysis. Environ Earth Sci 67(4):971–986. https://doi.org/10.1007/s12665-012-1539-9

Feng W, Wang C, Lei X, Wang H, Zhang X (2020a) Distribution of Nitrate content in groundwater and evaluation of potential health risks: a case study of rural areas in Northern China. Int J Environ Res Public Health. https://doi.org/10.3390/ijerph17249390

Feng WW, Qian H, Xu PP, Hou K (2020b) Hydrochemical Characteristic of groundwater and its impact on crop yields in the Baojixia Irrigation Area China. Water 12(5):18. https://doi.org/10.3390/w12051443

Gao Y, Qian H, Huo C, Chen J, Wang H (2020) Assessing natural background levels in shallow groundwater in a large semiarid drainage Basin. J Hydrol 584:124638. https://doi.org/10.1016/j.jhydrol.2020.124638

Guptha GC, Swain S, Al-Ansari N, Taloor AK, Dayal D (2021) Evaluation of an urban drainage system and its resilience using remote sensing and GIS. Remote Sens Appl: Soc Environ 23:100601. https://doi.org/10.1016/j.rsase.2021.100601

Guptha GC, Swain S, Al-Ansari N, Taloor AK, Dayal D (2022) Assessing the role of SuDS in resilience enhancement of urban drainage system: a case study of Gurugram City India. Urban Clim 41:101075. https://doi.org/10.1016/j.uclim.2021.101075

Hamdi M, Goïta K, Karaouli F, Zagrarni MF (2021) Hydrodynamic groundwater modeling and hydrochemical conceptualization of the mining area of Moulares Redeyef (southwestern of Tunisia): new local insights. Phys Chem Earth, Parts a/b/c 121:102974. https://doi.org/10.1016/j.pce.2020.102974

Hosseinifard SJ, Aminiyan MM (2015) Hydrochemical characterization of groundwater quality for drinking and agricultural purposes: a case study in Rafsanjan Plain Iran. Water Qual Expo Health 7(4):531–544. https://doi.org/10.1007/s12403-015-0169-3

Jebastina N, Arulraj GP (2018) Spatial prediction of nitrate concentration using GIS and ANFIS modelling in groundwater. Bull Environ Contam Toxicol 101(3):403–409. https://doi.org/10.1007/s00128-018-2406-5

Jianyao C, Taniguchi M, Guanqun L, Miyaoka K, Onodera S, Tokunaga T, Fukushima Y (2007) Nitrate pollution of groundwater in the Yellow River delta China. Hydrogeol J 15(8):1605–1614. https://doi.org/10.1007/s10040-007-0196-7

Kawo NS, Karuppannan S (2018) Groundwater quality assessment using water quality index and GIS technique in Modjo River Basin, central Ethiopia. J Afr Earth Sci 147:300–311. https://doi.org/10.1016/j.jafrearsci.2018.06.034

Khanoranga, Khalid S (2019) An assessment of groundwater quality for irrigation and drinking purposes around brick kilns in three districts of Balochistan province, Pakistan, through water quality index and multivariate statistical approaches. J Geochem Explor 197:14–26. https://doi.org/10.1016/j.gexplo.2018.11.007

Krishnakumar P, Lakshumanan C, Kishore VP, Sundararajan M, Santhiya G, Chidambaram S (2014) Assessment of groundwater quality in and around Vedaraniyam South India. Environ Earth Sci 71(5):2211–2225. https://doi.org/10.1007/s12665-013-2626-2

Li PY, Qian H, Howard KWF, Wu JH (2015) Building a new and sustainable "Silk Road economic belt." Environ Earth Sci 74(10):7267–7270. https://doi.org/10.1007/s12665-015-4739-2

Li PY, Wu JH, Qian H, Zhang YT, Yang NA, Jing LJ, Yu PY (2016a) Hydrogeochemical characterization of groundwater in and around a wastewater irrigated forest in the southeastern edge of the Tengger Desert Northwest China. Expo Health 8(3):331–348. https://doi.org/10.1007/s12403-016-0193-y

Li PY, Zhang YT, Yang NA, Jing LJ, Yu PY (2016b) Major ion chemistry and quality assessment of groundwater in and around a mountainous Tourist Town of China. Expo Health 8(2):239–252. https://doi.org/10.1007/s12403-016-0198-6

Li PY, He S, He XD, Tian R (2018) Seasonal hydrochemical characterization and groundwater quality delineation based on matter element extension analysis in a paper wastewater irrigation area Northwest China. Expo Health 10(4):241–258. https://doi.org/10.1007/s12403-017-0258-6

Luo Y, Wang HY (2019) Modeling the impacts of agricultural management strategies on crop yields and sediment yields using APEX in Guizhou Plateau, southwest China. Agri Water Manag 216:325–338. https://doi.org/10.1016/j.agwat.2019.01.018

Manassaram DM, Backer LC, Messing R, Fleming LE, Luke B, Monteilh CP (2010) Nitrates in drinking water and methemoglobin levels in pregnancy: a longitudinal study. Environ Health. https://doi.org/10.1186/1476-069x-9-60

Paladino O, Seyedsalehi M, Massabo M (2018) Probabilistic risk assessment of nitrate groundwater contamination from greenhouses in Albenga plain (Liguria, Italy) using lysimeters. Sci Total Environ 634:427–438. https://doi.org/10.1016/j.scitotenv.2018.03.320

Patel P, Thakur PK, Aggarwal SP, Garg V, Dhote PR, Nikam BR, Swain S, Al Ansari N (2022) Revisiting 2013 Uttarakhand flash floods through hydrological evaluation of precipitation data sources and morphometric prioritization. Geomat, Nat Hazards Risk 13(1):646–666. https://doi.org/10.1080/19475705.2022.2038696

Qian H, Li P, Howard KWF, Yang C, Zhang X (2012) Assessment of groundwater vulnerability in the Yinchuan Plain, Northwest China using OREADIC. Environ Monit Assess 184(6):3613–3628. https://doi.org/10.1007/s10661-011-2211-7

Qian H, Chen J, Howard KWF (2020) Assessing groundwater pollution and potential remediation processes in a multi-layer aquifer system. Environ Pollut 263:114669. https://doi.org/10.1016/j.envpol.2020.114669

Qiu J (2010) China faces up to groundwater crisis. Nature 466(7304):308–308. https://doi.org/10.1038/466308a

Quintanilla-Villanueva GE, Villanueva-Rodriguez M, Guzman-Mar JL, Torres-Gaytan DE, Hernandez-Ramirez A, Orozco-Rivera G, Hinojosa-Reyes L (2020) Mobility and speciation of mercury in soils from a mining zone in Villa Hidalgo, SLP, Mexico: a preliminary risk assessment. Appl Geochem. https://doi.org/10.1016/j.apgeochem.2020.104746

Raja V, Neelakantan MA (2021) Evaluation of groundwater quality with health risk assessment of fluoride and nitrate in Virudhunagar district, Tamil Nadu, India. Arabian J Geosci. https://doi.org/10.1007/s12517-020-06385-5

Ravikumar P, Aneesul Mehmood M, Somashekar RK (2013) Water quality index to determine the surface water quality of Sankey tank and Mallathahalli lake, Bangalore urban district, Karnataka India. Appl Water Sci 3(1):247–261. https://doi.org/10.1007/s13201-013-0077-2

Sahoo S, Swain S, Goswami A, Sharma R, Pateriya B (2021) Assessment of trends and multi-decadal changes in groundwater level in parts of the Malwa region, Punjab India. Groundw Sustain Dev 14:100644. https://doi.org/10.1016/j.gsd.2021.100644

Swain S, Mishra SK, Pandey A (2021) A detailed assessment of meteorological drought characteristics using simplified rainfall index over Narmada River Basin India. Environ Earth Sci. https://doi.org/10.1007/s12665-021-09523-8

Swain S, Sahoo S, Taloor AK (2022a) Groundwater quality assessment using geospatial and statistical approaches over Faridabad and Gurgaon districts of National Capital Region India. Appl Water Sci. https://doi.org/10.1007/s13201-022-01604-8

Swain S, Taloor AK, Dhal L, Sahoo S, Al-Ansari N (2022b) Impact of climate change on groundwater hydrology: a comprehensive review and current status of the Indian hydrogeology. Appl Water Sci. https://doi.org/10.1007/s13201-022-01652-0

Swain S, Mishra SK, Pandey A, Kalura P (2022c) Inclusion of groundwater and socio-economic factors for assessing comprehensive drought vulnerability over Narmada River Basin India: a geospatial approach. Appl Water Sci. https://doi.org/10.1007/s13201-021-01529-8

Tahmasebi P, Mahmudy-Gharaie MH, Ghassemzadeh F, Karouyeh AK (2018) Assessment of groundwater suitability for irrigation in a gold mine surrounding area, NE Iran. Environ Earth Sci. https://doi.org/10.1007/s12665-018-7941-1

Vasanthavigar M, Srinivasamoorthy K, Prasanna MV (2012) Evaluation of groundwater suitability for domestic, irrigational, and industrial purposes: a case study from Thirumanimuttar river basin Tamilnadu, India. Environ Monit Assess 184(1):405–420. https://doi.org/10.1007/s10661-011-1977-y

Ward MH, Jones RR, Brender JD, de Kok TM, Weyer PJ, Nolan BT, Villanueva CM, van Breda SG (2018) Drinking water nitrate and human health: an updated review. Int J Environ Res Public Health 15(7):31. https://doi.org/10.3390/ijerph15071557

WHO, G (2011) Guidelines for drinking-water quality. World Health Organization 216: 303-304

Wu J, Wang L, Wang S, Tian R, Xue C, Feng W, Li Y (2017) Spatiotemporal variation of groundwater quality in an arid area experiencing long-term paper wastewater irrigation, northwest China. Environ Earth Sci. https://doi.org/10.1007/s12665-017-6787-2

Wu J, Lu J, Wen XH, Zhang ZH, Lin YC (2019) Severe Nitrate pollution and health risks of coastal aquifer simultaneously influenced by saltwater intrusion and intensive anthropogenic activities. Arch Environ Contam Toxicol 77(1):79–87. https://doi.org/10.1007/s00244-019-00636-7

Xu PP, Feng WW, Qian H, Zhang QY (2019a) Hydrogeochemical characterization and irrigation quality assessment of shallow groundwater in the Central-Western Guanzhong Basin, China. Int J Environ Res Public Health 16(9):18. https://doi.org/10.3390/ijerph16091492

Xu PP, Li MN, Qian H, Zhang QY, Liu FX, Hou K (2019b) Hydrochemistry and geothermometry of geothermal water in the central Guanzhong Basin, China: a case study in Xi'an. Environ Earth Sci 78(3):20. https://doi.org/10.1007/s12665-019-8099-1

Xu PP, Zhang QY, Qian H, Li MN, Hou K (2019c) Characterization of geothermal water in the piedmont region of Qinling Mountains and Lantian-Bahe Group in Guanzhong Basin China. Environ Earth Sciences 78(15):17. https://doi.org/10.1007/s12665-019-8418-6

Xu P, Zhang Q, Qian H, Guo M, Yang F (2021a) Exploring the geochemical mechanism for the saturated permeability change of remolded loess. Eng Geol 284:105927. https://doi.org/10.1016/j.enggeo.2020.105927

Xu P, Zhang Q, Qian H, Yang F, Zheng L (2021b) Investigating the mechanism of pH effect on saturated permeability of remolded loess. Eng Geol 284:105978. https://doi.org/10.1016/j.enggeo.2020.105978

Zhang QY, Xu PP, Qian H (2019) Assessment of groundwater quality and human health risk (HHR) evaluation of nitrate in the Central-Western Guanzhong Basin, China. Int J Environ Res Public Health 16(21):16. https://doi.org/10.3390/ijerph16214246

Zhang Q, Xu P, Qian H, Yang F (2020a) Hydrogeochemistry and fluoride contamination in Jiaokou Irrigation District, Central China: Assessment based on multivariate statistical approach and human health risk. Sci Total Environ. https://doi.org/10.1016/j.scitotenv.2020a.140460

Zhang QY, Xu PP, Qian H (2020b) Groundwater quality assessment using improved water quality index (WQI) and Human Health Risk (HHR) Evaluation in a Semi-arid Region of Northwest China. Expo Health 12(3):487–500. https://doi.org/10.1007/s12403-020-00345-w

Zhang Q, Qian H, Xu P, Hou K, Yang F (2021a) Groundwater quality assessment using a new integrated-weight water quality index (IWQI) and driver analysis in the Jiaokou Irrigation District China. Ecotoxicol Environ Safety 212:111992. https://doi.org/10.1016/j.ecoenv.2021.111992

Zhang Q, Qian H, Xu P, Li W, Feng W, Liu R (2021b) Effect of hydrogeological conditions on groundwater nitrate pollution and human health risk assessment of nitrate in Jiaokou Irrigation District. J Clean Prod 298:126783. https://doi.org/10.1016/j.jclepro.2021.126783

Zhang Q, Xu P, Chen J, Qian H, Qu W, Liu R (2021c) Evaluation of groundwater quality using an integrated approach of set pair analysis and variable fuzzy improved model with binary semantic analysis: a case study in Jiaokou Irrigation District, east of Guanzhong Basin. China Sci Total Environ 767:145247. https://doi.org/10.1016/j.scitotenv.2021.145247